October 2003 • NREL/SR-520-34823

Subcontractor Report

Real Time Optics of the Growth of Textured Silicon Films in Photovoltaics

Final Technical Report
1 August 1999—12 August 2002

R.W. Collins and C.R. Wronski
The Pennsylvania State University
University Park, Pennsylvania

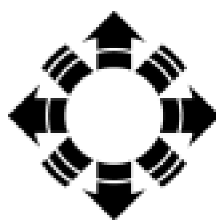

NREL

National Renewable Energy Laboratory

1617 Cole Boulevard
Golden, Colorado 80401-3393

NREL is a U.S. Department of Energy Laboratory
Operated by Midwest Research Institute • Battelle • Bechtel

Contract No. DE-AC36-99-GO10337

October 2003 • NREL/SR-520-34823

Real Time Optics of the Growth of Textured Silicon Films in Photovoltaics

Final Technical Report
1 August 1999—12 August 2002

R.W. Collins and C.R. Wronski
The Pennsylvania State University
University Park, Pennsylvania

NREL Technical Monitor: R. Matson

Prepared under Subcontract No. AAD-9-18668-09

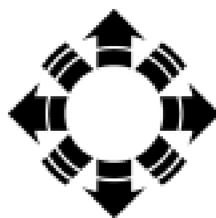

National Renewable Energy Laboratory

1617 Cole Boulevard
Golden, Colorado 80401-3393

NREL is a U.S. Department of Energy Laboratory
Operated by Midwest Research Institute • Battelle • Bechtel

Contract No. DE-AC36-99-GO10337

This publication was reproduced from the best available copy
Submitted by the subcontractor and received no editorial review at NREL

NOTICE

This report was prepared as an account of work sponsored by an agency of the United States government. Neither the United States government nor any agency thereof, nor any of their employees, makes any warranty, express or implied, or assumes any legal liability or responsibility for the accuracy, completeness, or usefulness of any information, apparatus, product, or process disclosed, or represents that its use would not infringe privately owned rights. Reference herein to any specific commercial product, process, or service by trade name, trademark, manufacturer, or otherwise does not necessarily constitute or imply its endorsement, recommendation, or favoring by the United States government or any agency thereof. The views and opinions of authors expressed herein do not necessarily state or reflect those of the United States government or any agency thereof.

Available electronically at http://www.osti.gov/bridge

Available for a processing fee to U.S. Department of Energy and its contractors, in paper, from:

U.S. Department of Energy
Office of Scientific and Technical Information
P.O. Box 62
Oak Ridge, TN 37831-0062
phone: 865.576.8401
fax: 865.576.5728
email: reports@adonis.osti.gov

Available for sale to the public, in paper, from:
U.S. Department of Commerce
National Technical Information Service
5285 Port Royal Road
Springfield, VA 22161
phone: 800.553.6847
fax: 703.605.6900
email: orders@ntis.fedworld.gov
online ordering: http://www.ntis.gov/ordering.htm

Printed on paper containing at least 50% wastepaper, including 20% postconsumer waste

Table of Contents

Abstract iv

I. Introduction 1

II. Optical Instrumentation Development 1
   A. Multichannel Stokes Vector Ellipsometry 2
   B. Multichannel Mueller Matrix Ellipsometry 4

III. Amorphous, Protocrystalline, and Microcrystalline Silicon Film Growth 7

IV. Optical Metrology of Photovoltaic Materials 8

V. Optical Modeling of a-Si:H-Based Solar Cells 10

VI. Conclusions and Future Directions 12

VII. Bibliography 14

Abstract

Novel optical instruments, including single and dual rotating-compensator multichannel ellipsometers have been designed and developed to probe the evolution of the microstructure, spectroscopic optical properties, and other materials characteristics during the fabrication and processing of individual thin films and thin film structures used in photovoltaic devices. These instruments provide a foundation for next-generation process design/control and metrology in existing and future photovoltaics technologies. In this project, the materials system studied in the greatest detail was thin film silicon, fabricated at low temperatures by plasma-enhanced chemical vapor deposition. Real time measurements of such thin films by multichannel ellipsometry have established deposition phase diagrams that provide guiding principles for multistep fabrication of high performance amorphous (a-Si:H) and microcrystalline (μc-Si:H) solar cells. Such phase diagrams have also served to disprove conventional wisdom in the fabrication of thin film solar cell structures, thus avoiding future unproductive research efforts.

In addition, a combination of the novel real time and ex situ optical measurements have provided databases of analytical formulas for the spectroscopic optical properties of thin film and bulk materials used in amorphous and microcrystalline silicon thin film photovoltaics technologies. Such databases include, for example, amorphous silicon-based alloys of any pre-specified optical band gap, the transparent conducting oxide (TCO) films and superstrate glasses used by industry, and the metallic retro-reflecting materials. This database can be applied in optical modeling of the device structures used in these technologies, and in next generation optical engineering for maximum collection of incident solar irradiance. As examples of the approach, we have highlighted how microscopic roughness at the TCO/p-layer interface acts as an antireflecting layer for enhanced collection in p-i-n structures and how intermixing at the ZnO/Ag interface in retro-reflectors act as a parasitic absorber for reduced collection.

I. Introduction

Much of the process development for materials fabrication as well the optical device design in thin film photovoltaics technologies have been undertaken using trial and error approaches. Even so, such approaches have led to rapid progress in the initial stages of several new technologies. However as technologies become too mature or as processing procedures become too complex for trial and error approaches, new analytical tools are needed so that improvements in current and future generation technology can be driven by a detailed scientific understanding of the materials and how they are assembled. Furthermore, if thin film photovoltaics is to be a serious contender for electric power generation on a larger scale, key optical metrologies are needed for in-line process monitoring and control of module fabrication. In the same way that numerous such metrologies have been developed along with the microelectronics industry to support its continued advancement, there will be a corresponding need for metrologies in the photovoltaics industry. At this time, however, the development and application of such tools in thin film photovoltaics remain in their infancy. The goal of this project has been to address this important need in two important ways.

First, high speed optical instrumentation based on advanced forms of multichannel ellipsometry, i.e., Stokes vector and Mueller matrix spectroscopy, have been developed for the first time. One advantage of these new approaches the ability to analyze multilayered stacks that exhibit both microscopic and macroscopic structure, as well as optical and structural anisotropy, complexities that are prevalent in thin film devices. Another advantage of these approaches is the ability to perform high speed spectroscopy during materials fabrication that allows one to deduce the evolution of the phase, structure, and optical properties versus film thickness. This has led to the development of phase diagrams that can guide multistep fabrication of optimized devices. Second, the spectroscopic optical properties extracted in real time analyses, in conjunction with results from ex situ measurements, provide a very useful database for advanced optical modeling and engineering of current and future generation devices.

II. Optical Instrument Development

In this project, novel multichannel optical instruments have been developed that provide the capability of probing the fabrication of photovoltaic structures in real time. The goal of this aspect of the research is to extract the maximum possible information from a real time optical measurement so that spectroscopic optical properties, microstructure and macrostructure, composition, and even temperature of the materials can be characterized from the data collected

throughout the deposition process. To meet this goal, multichannel spectroscopic ellipsometers with increasing real time measurement capabilities have been developed.

In the first half of this project, the single rotating-compensator multichannel ellipsometer was designed and developed, applying a previous expertise base established through the perfection of a state-of-the-art rotating-polarizer multichannel ellipsometer with a spectral range from 1.5 to 6.5 eV. The single rotating-compensator instrument provides the spectroscopic 4x1 Stokes vector (1.5 to 4.7 eV) of the beam reflected from the sample surface during its preparation and/or processing with a minimum full spectra acquisition time of ~50 ms. In the second half of this project, the dual rotating-compensator multichannel ellipsometer was designed and developed, building on the expertise obtained in the first half. The dual rotating compensator instrument provides the spectroscopic 4x4 Mueller matrix (1.5 to 4.7 eV) of the sample surface during its preparation and/or processing with a minimum full spectra acquisition time of ~0.25 s.

A detailed description with schematics of the multichannel ellipsometry development supported by this project is listed as Bibliography item [47]. This article will appear in "*Handbook of Ellipsometry*" edited by Harland G. Tompkins and Eugene A. Irene to be published by Noyes later in 2003. In the next subsections additional details are provided for each of these two instrument configurations specific to applications in solar energy materials and device development.

A. Multichannel Stokes Vector Ellipsometry

In multichannel Stokes vector ellipsometry, a collimated white light source followed by a fixed polarized is mounted on the polarization generation arm of the instrument, and a (rotating compensator)/(fixed polarizer) pair is mounted on the polarization detection arm of the instrument to accept the specularly reflected beam. Thus, linearly polarized light with coherent and orthogonal *p* and *s* components (i.e., with the electric fields parallel and perpendicular to the plane of incidence, respectively) is directed onto the sample, and the amplitudes and phases of these polarization components are modified upon specular reflection. The sample may also depolarize the probe beam, e.g., if it is inhomogeneous on a scale greater than the lateral coherence length of the beam. The (rotating compensator)/(fixed polarizer) pair analyzes this polarization modification and possible depolarization at all wavelengths simultaneously, and the resulting modulated white light beam from this pair is dispersed onto a linear photodiode array for waveform analysis. The photodiode array is read out 8 times per optical cycle π/ω_C (or one-half mechanical cycle), where $\omega_C/2\pi \sim 10$ Hz is the mechanical rotation frequency of the compensator. From these 8 read outs, spectra in the dc Fourier coefficient I_0 and the first (3 cosine, 4 sine) $2n\omega_B$ Fourier coefficients (α_{2n}, β_{2n}) (normalized to the dc coefficient) can be

determined. Only the spectra in the dc coefficient and those coefficients with n=1 and 2, i.e., $\{I_0, (\alpha_2, \beta_2), (\alpha_4, \beta_4)\}$ are non-zero for the most general sample. From these five spectra, the reflected beam polarization state characteristics (i.e., the Stokes vector elements) are obtained, and from these characteristics optical and structural characteristics of the sample are extracted.

In fact, the incorporation of a (rotating compensator)/(fixed polarizer) pair as a polarization state detector after the sample allows one to extract the full Stokes vector of the reflected light beam. The Stokes vector of the beam is a 4x1 column vector that encodes four different characteristics: (i) the tilt angle Q ($-90° < Q \leq 90°$) of the ellipse of polarization, measured from the plane of incidence in a counterclockwise-positive sense, looking opposite to the beam direction; (ii) the ellipticity angle $\chi = \tan^{-1} e$ ($-45° \leq \chi \leq 45°$; $-1 \leq e \leq 1$) of the ellipse of polarization, where e is the ellipticity, i.e., the semiminor-to-semimajor axis ratio of the ellipse; (iii) the irradiance in the reflected beam I_r normalized to that in the incident beam I_i and (iv) the degree of polarization p ($0 \leq p \leq 1$). These four Stokes vector characteristics, denoted collectively as $\{(Q, \chi), p, I_r/I_i\}$, provide different types of information on the sample.

For a specular, macroscopically uniform (hence non-depolarizing) sample, (Q, χ) provide information on the thicknesses, compositions (for alloys or microscopically-mixed phases), and optical properties of the layers that comprise the sample. In this case of a "perfect sample", p is unity and I_r/I_i provides no further information about the sample than is inherent in (Q, χ). Thus, the multichannel Stokes vector ellipsometer in turn provides no further information in comparison with the conventional rotating-polarizer multichannel ellipsometer developed earlier. If the sample is macroscopically non-uniform, however, different regions of the sample illuminated by the probe beam lead to different polarization modifications. When the scale of the non-uniformity is larger than the lateral coherence length of the beam, then the resulting reflected beam exhibits a superposition of irradiances in different polarization states so that $p < 1$. In this case, I_r/I_i can be used along with p as additional independent measurements for analysis of the sample properties. Thus, the full set of Stokes vectors parameters $\{(Q, \chi), p, I_r/I_i\}$ can be used to extract information, not only on the thicknesses and microscopic structure, but also on the macroscopic structure of the sample. Further discussion regarding the characterization of the sample on different scales is warranted and will be given next.

The dividing line between microscopic and macroscopic from an optical standpoint is $\sim\lambda/10$ or ~500 Å. For smaller structural scales, no significant depolarization occurs (p=1), non-specular scattering is negligible, and effective medium theories can be used to analyze the structure and optical properties of roughness layers and mixed phases. For larger structural scales, p can decrease from unity and will then depend on the probe wavelength. For example when non-specular scattering occurs, the irradiance ratio I_r/I_i is lower than that predicted from a perfect microscopic model. In fact, the difference between the "perfect sample" irradiance ratio

and that observed experimentally provides the irradiance due to integrated scattering over all solid angles. Thus, this difference provides information on the macroscopic structure that leads to the scattering. In addition if any non-specular scattered light enters the detection system optics, it will register as a different polarization state, incoherent relative to the specular beam; so $p<1$. In this case, the spectral dependence of p can provide information on the scattering at the detected angle, and hence additional information on the macroscopic structure. If the sample is specular (non-scattering), but macroscopically non-uniform (e.g., exhibiting a thickness gradient) and if this non-uniformity scale is less than the lateral coherence length of the light (typically within the range of 1-10 μm), then the electric fields add and generate a pure polarization state (with $p=1$) that encodes information on the non-uniformity within $\{(Q, \chi), I_r/I_i\}$. In contrast if the non-uniformity scale of the specular sample is greater than the lateral coherence length, then the irradiances add and generate a mixed polarization state (with $p<1$) that encodes information on the non-uniformity within the entire Stokes vector $\{(Q, \chi), p, I_r/I_i\}$.

Samples that include non-specularity and non-uniformities on a wide range of scales are difficult to analyze to be sure, but the following summary provides the most useful associations:

Specular sample, microscopic structure (scale: L<500 Å):	(Q, χ)
Specular sample, macroscopic non-uniformity (scale: $0.1 < L < 1$ μm):	(Q, χ)
Specular sample, macroscopic non-uniformity (scale: $L > 10$ μm):	(Q, χ), p
Non-specular sample, macroscopic non-uniformity (scale: $0.1 < L < 1$ μm):	(Q, χ), I_r/I_i
Non-specular sample, macroscopic non-uniformity (scale: $L > 10$ μm):	(Q, χ), I_r/I_i, p.

This list describes the characteristics of the Stokes vector that are used to extract sample structure on different scales. Such optical analyses are difficult because each different type of sample structure requires a different analysis program, and often when a solution is obtained, its uniqueness is unclear. As a result, in an ex situ mode of operation, it is important to correlate the results of Stokes vector ellipsometry measurements with those of direct structural measurements such as profilometry, scanning electron microscopy, cross sectional transmission electron microscopy, and scanning tunneling and/or atomic force microscopy. Once the analysis approach is verified for a series of similar samples, then Stokes vector ellipsometry can be used effectively as a routine tool for real time analysis of materials fabrication and processing.

B. Multichannel Mueller Matrix Ellipsometry

The disadvantage of multichannel Stokes vector ellipsometry is the difficulty of extracting information when the (multilayer sample)/substrate system is anisotropic, i.e., the optical and

structural characteristics of one or more of the layers depends on the electric field direction in the layer. Optically isotropic systems include layers that are truly amorphous, or those that are cubic single crystalline, or even lower symmetry microcrystalline with a random distribution of grain orientations. Optically anisotropic systems include single crystal layers of lower symmetry than cubic, or layers that are amorphous, cubic crystalline, or randomly-oriented microcrystalline but with anisotropic microscopic or macroscopic structure. For anisotropic samples in low symmetry optical configurations, the linearly polarized *p* and *s* states are no longer the polarization eigenmodes, i.e., the states that remain unchanged upon reflection. Thus, incident *p* polarized light generates an *s* polarized component in the reflected beam and vice versa. In order to measure the cross-polarization amplitude reflection coefficients, and thus obtain additional information on anisotropic samples, the first multichannel Mueller matrix ellipsometer has been developed as part of this research effort.

In multichannel Mueller matrix ellipsometry, a collimated white light source is modulated by a (fixed polarizer)/(rotating compensator) pair on the polarization generation arm of the instrument, and a (rotating compensator)/(fixed polarizer) pair is used as well on the polarization detection arm of the instrument. Thus, the sample is exposed not only to linearly polarized light (as in the Stokes vector ellipsometer), but also to a wide variety of elliptical polarization states (i.e., with the coherent *p* and *s* component electric fields having differing amplitude ratios and phase differences). The (rotating compensator)/(fixed polarizer) pair on the detection side of the instrument analyzes the polarization modification and depolarization induced by the sample, at all wavelengths simultaneously. The resulting modulated white light beam from this pair is dispersed onto a linear photodiode array for waveform analysis. In this dual-rotating compensator configuration, the compensators on the polarization generation and detection sides of the instrument are rotated synchronously at $5\omega_B$ and $3\omega_B$, respectively, where ω_B is the fundamental mechanical frequency. The photodiode array is read out 36 times per optical cycle π/ω_B (or one-half mechanical cycle), where $\omega_B/2\pi \sim 2$ Hz for the particular instrument design in this study. From these 36 read outs, spectra in the dc Fourier coefficient I_0 and the first (17 cosine, 18 sine) $2n\omega_B$ Fourier coefficients $(\alpha_{2n}, \beta_{2n})$ (normalized to the dc coefficient) can be determined. Only the spectra in the dc coefficient and a subset of the other coefficients given collectively by $\{I_0, (\alpha_{2n}, \beta_{2n}); n=1, 2, 3, 4, 5, 6, 7, 8, 10, 11, 13, \text{and } 16\}$ are non-zero for the most general sample. From these 25 spectra, the general anisotropic sample characteristics (i.e., the Mueller matrix elements) are obtained, and from the Mueller matrix, optical and structural characteristics of the sample can be extracted.

In optical metrology, the Mueller matrix of a given sample is the 4x4 matrix that premultiplies the incident beam 4x1 Stokes vector to predict the reflected beam 4x1 Stokes vector. So in contrast to the Stokes vector ellipsometer that provides the four parameters

describing the general polarization state of the reflected beam, the Mueller matrix ellipsometer provides the sixteen elements describing how the sample modifies the incident polarization state. This more general approach to multichannel ellipsometry is only possible by modulating the polarization state of the incident beam and detecting the reflected beam with a "polarimeter" (e.g., a rotating compensator and fixed polarizer pair). It is possible to deduce all sixteen elements of the Mueller matrix only for certain ratios of the two compensator rotation frequencies. In the instrument development reported here, the ratios 5:*m* (*m*=1, ..., 4) were considered, and the 5:3 ratio was selected as a compromise between the desirable increase in dc motor stability that occurs with increasing *m* and the undesirable increase in the highest frequency component of the waveform that also occurs with increasing *m*.

For anisotropic, non-depolarizing samples in the most general low symmetry measurement configuration, six parameters can be deduced from the Mueller matrix. These include the real and imaginary parts of the complex amplitude reflection ratios $\rho_{pp} \equiv r_{pp}/r_{ss}$, $\rho_{ps} \equiv r_{ps}/r_{ss}$, and $\rho_{sp} \equiv r_{sp}/r_{ss}$, where r_{ij} denotes the complex amplitude reflection coefficients defined by $r_{ij}=(E_j)_r/(E_i)_i$. In this latter expression, E denotes the complex electric field component, the inner subscript denotes the field direction (p or s) and the outer subscript denotes the reflected (r) or incident (i) waves. From the six parameters, for a bulk crystal it is possible to deduce the three principal complex dielectric functions (that define the dielectric tensor) corresponding to the normal mode directions of the fields (assuming that the crystal surface is in a known, appropriate low symmetry plane). More often one works with thin films in which a low symmetry configuration is not accessible, and sensitivity to the dielectric tensor is lost for fields along certain directions in the film (e.g., normal to the film surface in a high index material). Obviously in this latter case, extensive data analysis is required to extract the film thicknesses, the dielectric tensor orientation, and the film optical properties. Even for these "perfect film" situations, data analysis can be quite demanding. The problem becomes even more difficult for anisotropic, depolarizing samples in which the number of parameters that define the Mueller increases above six. The one advantage in measuring the full Mueller matrix is that there are multiple ways to extract useful parameters so that the measurables are well defined; however, the development of analysis techniques to interpret these measurables remains in its infancy.

In this research, the simplest material systems have been studied first and more complicated systems are being considered in a step-by-step fashion. The first system of interest was (110) Si in which case the first simultaneous real time measurement of bulk isotropic and surface anisotropic complex dielectric function spectra have been performed. This work has been described in an article published in *Physical Review Letters* in 2003 listed as item [48] in the Bibliography. A more extensive description has also been submitted to *Review of Scientific Instruments*, listed as item [47]. The next step in this ongoing research is to characterize

anisotropy in nano- and micro-scale sculptured thin films fabricated by oblique angle deposition in conjunction with substrate rotation. The third step in the research is to characterize non-uniform isotropic and anisotropic surfaces that scatter light.

III. Amorphous, Protocrystalline, and Microcrystalline Silicon Film Growth

Real time spectroscopic ellipsometry (RTSE) has been applied in the single rotating-compensator multichannel configuration in order to develop deposition phase diagrams that can guide the fabrication of hydrogenated silicon (Si:H) thin films by plasma-enhanced chemical vapor deposition (PECVD) at low temperatures (<300°C) for highest performance solar cells. The simplest phase diagrams incorporate a single transition from the amorphous growth regime to the mixed-phase (amorphous + microcrystalline) growth regime versus accumulated film thickness [the $a \rightarrow (a+\mu c)$ transition]. These phase diagrams have shown that optimization of amorphous silicon (a-Si:H) intrinsic (i) layers by rf plasma-enhanced chemical vapor deposition (PECVD) at low rates is achieved using *protocrystalline* Si:H. This material is deposited with the maximum possible flow ratio of H_2 to SiH_4 that can be sustained while avoiding the $a \rightarrow (a+\mu c)$ transition that inevitably occurs for film thicknesses greater than the desired value in the device. More recent studies have suggested that a similar strategy is appropriate for the optimization of p-type Si:H thin films.

Thus, the ability to characterize the phase evolution of the i and p-layers incorporated into a-Si:H and microcrystalline silicon (μc-Si:H) thin film solar cells is critically important for cell optimization. In this research, a new method has been established to extract the thickness evolution of the μc-Si:H volume fraction in mixed-phase amorphous + microcrystalline silicon [(a+μc)-Si:H] i-layers. This method is based on RTSE measurements performed during PECVD of the Si:H films, coupled with a novel virtual interface approach for RTSE analysis. As a result, one can identify—in addition to the evolution of the microcrystalline fraction—the thickness at which crystallites first nucleate from the a-Si:H phase, as well as the thickness at which they coalesce to form single-phase μc-Si:H in the growth process. From these characteristics, the nucleation density and microcrystallite cone angle can be estimated assuming a crystallite cone growth model, and these latter parameters show excellent agreement with direct structural and electronic device measurements.

The simple phase diagrams can be extended to include in addition the thickness at which a roughening transition is detected in the amorphous film growth regime. In general this roughening transition thickness shifts to larger values with increasing flow ratio of H_2 to SiH_4, and with increasing substrate temperature in the range 200-300°C (as long as the films remain amorphous throughout). In fact, optimized films for the i-layers of solar cells exhibit smooth,

stable surfaces without a roughening transition even throughout the growth of films as thick as 4000 Å. Results are presented consistent with the suggestion that when the roughening transition occurs at greater thickness values, the diffusion length of adsorbed precursors is enhanced. Unfortunately, the roughening transition shifts rapidly to smaller values with an increase in rf plasma power that increases the a-Si:H deposition rate. It is proposed that optimization of a-Si:H in higher rate PECVD processes requires finding a set of conditions leading to the maximum possible thickness onset for the amorphous roughening transition. Based on this guidance, a novel approach that combines elevated pressure and plasma power levels has been proposed.

Item [51] of the Bibliography provides an in-depth review of how real time spectroscopic ellipsometry in the single rotating-compensator multichannel configuration has been used to establish guiding principles for the fabrication of Si:H thin film components in solar cells. This review is to be published as an article in Solar Energy Materials and Solar Cells in 2003.

IV. Optical Metrology of Photovoltaic Materials

In thin film photovoltaic technologies, multilayer stacks incorporating as many as a dozen layers may be deposited to complete the solar cell structure. Layers are incorporated for multiple purposes including photocarrier generation, separation, and collection. For example, in a-Si:H technology, tandem or triple-junction solar cells incorporate two or three absorber layers having optical band gaps spanning the range from 1.3 to 1.9 eV that serve to collect light from different regions of the solar spectrum. Stepwise or continuous hydrogen-tailoring and alloy-grading are sometimes used in the absorber layers in order to enhance photon absorption and photocarrier separation. In addition, four or six very thin doped layers are incorporated for photocarrier separation and collection. As a result, the complexities of thin film solar cell structures lead to difficulties in the optimization of cell efficiency through empirical variations of layer and material parameters such as thicknesses and compositional profiles.

For guidance in solar cell optimization, sophisticated computer programs such as AMPS developed at The Pennsylvania State University and PVOptics developed at the National Renewable Energy Laboratory have been applied to simulate the separate electronic and optical aspects of cell performance. Optically-based programs can be applied to predict the spectroscopic reflectance, absorbance, and transmittance losses, and to establish the optical quantum efficiency due to absorption in each absorber layer. By combining the predicted optical quantum efficiencies of all the absorber layers, one obtains the quantum efficiency of the overall solar cell that would result if each electron-hole pair generated within an absorber layer is separated and collected. The electronically-based program then allows one to compute

recombination losses and, thereby, to convert optical generation profiles in the absorber layers to the predicted electronic quantum efficiency.

In general, the optically-based simulation programs require a large volume of input data, specifically the optical properties, i.e., the index of refraction and extinction coefficient spectra (n, k), of all the possible layer components of the device including, as well, the variations in these properties with composition for any tailored or graded layers. As a result, it is generally not possible to extract information (e.g., layer thicknesses and component material band gaps or compositions) directly through non-linear least-squares regression analysis of experimental measurements such as the spectroscopic reflectance and electronic quantum efficiency. Thus, these programs are generally not used for fitting data—only for simulating data, whereby layer and material inputs are provided and the optical or electronic behavior is predicted for qualitative comparisons with experimental data. The accuracy of such simulations is limited by the accuracy of the input parameters, however. In this research, we describe the development of an input database that defines the spectra in the optical properties of all the materials used in a-Si:H solar cell technology. Item [18] of the Bibliography provides a detailed description of the database development. This article appears in the collection "*Photovoltaics for the 21st Century II*" edited by R. D. McConnell and V. K. Kapur and published by the Electrochemical Society (Pennington NJ, 2001, pp. 199-228).

In the case of amorphous silicon technology, the greatest difficulty arises from the need to establish optical properties for materials of arbitrarily-chosen optical band gaps over the 1.3 - 1.9 eV range. In this research, a Kramers-Kronig consistent analytical expression has been developed to fit the measured optical properties of a discrete set of solar cell quality a-Si:H-based alloys. The analytical expression incorporates the minimum number of physically meaningful, E-independent parameters required to fit (n, k) versus E. The fit is performed simultaneously throughout the following three regions: (i) the sub-bandgap (or Urbach tail) region where the absorption coefficient α increases exponentially with E, (ii) the near-bandgap region where transitions are assumed to occur between parabolic bands with constant dipole matrix element, and (iii) the above-bandgap region where (n, k) can be simulated assuming a single Lorentz oscillator. One starts by plotting the best fit parameters as a function of optical band gap (as measured by a routine method such as transmission and reflection spectroscopy) for the discrete set of alloys. These plots are fit in turn to simple polynomial relations that allow one to interpolate between band gaps and reach the stated goal, namely to establish the parameter set relevant for computing the (n, k) spectra of an a-Si:H alloy of arbitrarily-chosen optical band gap. The details of this effort are provided in item [32] of the Bibliography, a comprehensive article appearing in *Journal of Applied Physics* (vol. 92, 2002, pp. 2424-2436).

V. Optical Modeling of a-Si:H-Based Solar Cells

Extensive optical measurements have demonstrated that microscopic surface and interface roughness is pervasive in amorphous silicon (a-Si:H) based materials and device structures and exerts considerable influence on their specular reflection properties. Such roughness exists on the surfaces of nominally specular and textured substrates, as well as at each of the interfaces between the components of the multilayer stack used in photovoltaics devices. As noted earlier, microscopic roughness is defined as surface/interface modulations with an in-plane scale at least an order of magnitude smaller than the wavelength λ of the incident light beam, i.e., less than ~500 Å. The optical effect of microscopic interface roughness can be simulated by inserting a layer at the interface whose thickness scales with the root-mean-square roughness and whose optical properties are determined from the Bruggeman effective medium theory assuming a composite of the overlying and underlying materials. In contrast, macroscopic roughness is defined as modulations with in-plane correlation lengths within an order of magnitude of λ or larger. The optical effect of macroscopic roughness at an interface is a reduction in the specularly reflected and transmitted electric field amplitudes, (e.g., in accordance with scalar diffraction theory). This reduction is offset by non-specularly scattered field components in the reflected and transmitted waves.

In simulations of the optical quantum efficiency (QE) of a-Si:H-based solar cells, the complicated light-trapping effects of macroscopic roughness have been widely considered; yet the simpler effects of microscopic roughness have been widely ignored. In this research, we have explored for the first time the effects of transparent conducting oxide interface layers in the a-Si:H solar cell structure on the simulated optical QE. Here, the nature of the interface layers are deduced independently from ex situ, in situ, and real time spectroscopic ellipsometry (SE) of photovoltaic structures, and the effects of these layers on the QE of the solar cell are determined. This approach is in contrast to the usual one for optical modeling in which inputs of the simulation routines are chosen to yield outputs in qualitative agreement with experimental QE curves. The latter approach should not be considered reliable unless the simulation routines include the complete optical physics of the problem.

We have analyzed ex situ, in situ, and real time SE data for a-Si:H-based structures in order to establish inputs for optical modeling of solar cells, focusing on the effects of non-idealities at the interfaces of the transparent conducting oxides. The first non-ideality considered in this research is microscopic roughness at the SnO_2/p/i interface in the p-i-n solar cell. In this study, two different SnO_2 layers were studied. The first was textured Asahi U-type, doped SnO_2 on glass. This film exhibits the maximum surface microroughness layer thickness in this study (450 Å), leading in turn to the maximum interface roughness when the p-i-n cell is deposited on

its surface. The second layer was a thin specular, doped SnO_2 on a silicon wafer prepared by BP Solar; its microroughness layer is much thinner (105 Å). The second non-ideality considered here occurs at the ZnO/Ag back-reflector interface, due to combined effects of microroughness and chemical intermixing. In this case, a specular ZnO/Ag/(stainless steel) structure prepared by United Solar was studied. For this structure, the steel was optically polished prior to the sputter depositions in order to minimize microroughness at the ZnO/Ag interface and lead to a dominant chemically intermixed layer (70 Å).

Multilayer optical modeling has been applied assuming incoherent multiple reflections within the glass superstrate of the p-i-n solar cell structure and coherent reflections within all other layers, in order to compute the optical QE, i.e., the fraction of incident photons absorbed in the i-layer vs. wavelength, for the single-junction solar cell. Because the retro-reflecting Ag film is opaque, photons that are not absorbed in the i-layer will either be absorbed in the other layers and lost, or reflected from the entire structure and lost. The Kramers-Kronig consistent database described in Sec. IV is applied for the optical properties of the a-Si:H-based p, i, and n layers.

One effect of microroughness at interfaces in general is a dampening of the interference fringes. This result demonstrates that microroughness must be included in any optical model that attempts to quantify this phenomenon. More importantly, the net effect of the microroughness at interfaces is to increase the total photon flux collected by the i-layer, with the maximum gain in absorbance occurring at 550 nm. This gain provides a potential increase in short circuit current ΔJ_{sc} of the solar cell of ~0.2 mA/cm^2 for the specular SnO_2 (with 105 Å microroughness) and ~0.7 mA/cm^2 for the textured SnO_2 (with 450 Å microroughness) solely due to the effect of these roughness layers. The results were computed by integrating the product of the optical QE and the AM 1 spectral photon flux over the range from 270 to 900 nm. The optical gains associated with the microscopically rough layers are attributed to the suppression of refractive index discontinuities that lead to a suppression in the reflected irradiance. The dominant effect occurs at the SnO_2/p-layer interface where the refractive index discontinuity is the largest and the roughness layer thickness is the greatest. Thus, the microroughness acts as an anti-reflecting layer for this interface; photon flux that would otherwise be reflected from the p-layer in an ideal structure passes into the i-layer where it can be collected.

The loss associated with absorbance (i.e., the fraction of incident irradiance absorbed) in the ZnO/Ag interface region has also been determined. In this case, the largest absorbance loss occurs within the spectral range of 500-700 nm. Below 500 nm, the decrease in interface absorbance is attributed to the fact that almost all the incident irradiance is absorbed by the overlying structure such that very little reaches the ZnO/Ag interface. In contrast, the decrease above 700 nm is an apparent effect of the optical properties of the interlayer. This latter effect is expected to be strongly dependent on the chemical and microstructural nature of the ZnO/Ag

interlayer. If all parasitic losses at the ZnO/Ag could be converted to useful current, the potential gain in J_{sc} integrated from 270 to 900 nm, ranges from 0.4 mA/cm^2 for a chemically mixed interface layer 70 Å thick to 0.55 mA/cm^2 for a mixed interface layer 140 Å thick.

Thus, the combined results suggest that the effects of non-ideal interfaces on optical collection in a-Si:H solar cells can be significant, and potential current gains can be achieved by optimizing anti-reflection characteristics and minimizing parasitic back-reflector absorption losses. Deatils of these results are presented in item [23] of the Bibliography.

VI. Conclusions and Future Directions

This report details the results of an ambitious project covering state-of-the-art optical instrumentation design and construction, fundamental thin film growth investigations, solar cell fabrication process design, Kramers-Kronig consistent optical property determinations, optical database development, and optical modeling and engineering for enhanced collection in thin film solar cells.

* In optical instrumentation development, the first multichannel Stokes vector and Mueller matrix ellipsometers were designed and developed. These instruments provide increasing power in the analysis of textured (macroscopically structured) and anisotropic thin films. In future work, improved methods of optical data analysis are required for the simultaneous determination of microstructural, macrostructural, and optical property information, particularly for the anisotropic material systems.

* In fundamental studies of optimized amorphous silicon (a-Si:H) based thin film growth processes, a new regime of film growth yielding material called "protocrystalline" silicon has been identified. This material is amorphous in nature, but exhibits increased order and stability against light-induced degradation in comparison with conventional materials. In fact, protocrystalline silicon is prepared at the maximum possible H_2 to SiH_4 gas flow ratio R that can be sustained without entering the mixed-phase amorphous + microcrystalline growth regime. In the future, more detailed higher resolution structural studies are needed to determine if these protocrystalline films incorporate small nanocrystallites or medium range ordering. In addition, it is important to extend the concept of protocrystallinity to a-$Si_{1-x}Ge_x$:H narrow gap alloys for improved solar cell performance.

* In this research, guiding principles have been established for the optimization of a-Si:H solar cells. It has been found that both the p-layer and the i-layer in a-Si:H solar cell fabrication should be prepared at the maximum possible R while remaining within the protocrystalline growth regime. This approach has led to the highest open circuit voltage, highest fill factor, and highest stability under light induced degradation. Although the fabrication of single step p-layers

and two-step i-layers have been perfected, additional work needs to be done in developing multistep and continuously variable hydrogen dilution processing. Such advances have been made difficult by the large hysteresis in the deposition of Si materials across the phase diagram. In other words, once mixed-phase silicon is initiated at high R, one must decrease R significantly in order to suppress its continued development.

*   Kramers-Kronig (K-K) consistent optical models have been developed for a-Si:H and μc-Si:H-based materials for solar cells, as well as the other solar cell components including superstrate glasses, doped SnO_2, and back reflector metals. These models have been applied to experimental data collected by different methods including dual-beam photoconductivity, transmission and reflection spectroscopy and spectroscopic ellipsometry; and as a result extensive databases have been developed. Future efforts in the development of a K-K consistent optical model for zinc oxide are needed. This material plays important roles as a possible atomic H resistant top transparent conducting oxide (TCO) for superstrate p-i-n solar cells and as the dielectric spacer in retro-reflecting structures. Thus, more detailed studies and parameterization of its optical properties are warranted.

*   Optical modeling has demonstrated that the abruptness of interfaces on a microscopic scale has an important impact on the quantum efficiencies of a-Si:H based solar cells. Microscopic roughness can play a positive role as an antireflecting layer at the TCO/p-layer interface that allows more light to enter into the cell for absorption by the i-layer. Microscopic roughness can also play a negative role as a parasitic absorbing layer at the ZnO/metal interface at the back of the retro-reflecting structure. This latter role suggests that significant gains may be made through redesign of the retro-reflector. Future efforts also require incorporation of macroscopic roughness at interfaces into the optical model in order to optimize the collection of light through proper design of the multilayer stacks and their macroscopic structure.

VII. Bibliography

1. "Real Time Analysis of Amorphous and Microcrystalline Silicon Film Growth by Multichannel Ellipsometry", R. W. Collins, Joohyun Koh, A. S. Ferlauto, P. I. Rovira, Yeeheng Lee, R. J. Koval, and C. R. Wronski, Thin Solid Films 364, 129-137 (2000).

2. "Recent Progress in Thin Film Growth Analysis by Multichannel Spectroscopic Ellipsometry", R. W. Collins, H. Fujiwara, Joohyun Koh, P. I. Rovira, A. S. Ferlauto, J. A. Zapien, C. R. Wronski, and R. Messier, Applied Surface Spectroscopy 154, 217-228 (2000).

3. "Modeling the Dielectric Functions of Silicon-Based Films in the Amorphous, Nanocrystalline, and Microcrystalline Regimes", A. S. Ferlauto, Joohyun Koh, P. I. Rovira, C. R. Wronski, R. W. Collins, and Gautam Ganguly, Journal of Non-Crystalline Solids 266, 269-273 (2000).

4. "Optics of Textured Amorphous Silicon Surfaces", P. I. Rovira, A. S. Ferlauto, Joohyun Koh, C. R Wronski, and R. W. Collins, Journal of Non-Crystalline Solids 266, 279-283 (2000).

5. "Evolutionary Phase Diagrams for the Deposition of Silicon Thin Films from Hydrogen-Diluted Silane", Joohyun Koh, A. S. Ferlauto, P. I. Rovira, R. J. Koval, C. R. Wronski, and R. W. Collins, Journal of Non-Crystalline Solids 266, 43-47 (2000).

6. "Assessment of Effective-Medium Theories in the Analysis of Nucleation and Microscopic Surface Roughness Evolution for Semiconductor Thin Films", H. Fujiwara, Joohyun Koh, P. I. Rovira, and R. W. Collins, Physical Review B 61, 10832-10844 (2000).

7. "Multichannel Ellipsometer for Real Time Spectroscopy of Thin Film Deposition from 1.5 to 6.5 eV", J. A. Zapien, R. W. Collins, and R. Messier, Review of Scientific Instruments 71, 3451-3460 (2000).

8. "Multichannel Mueller Matrix Ellipsometer for Real-Time Spectroscopy of Anisotropic Surfaces and Films", Joungchel Lee, Joohyun Koh, and R. W. Collins, Optics Letters 25, 1573-1575 (2000).

9. "Dependence of Open-Circuit Voltage in Hydrogenated Protocrystalline Silicon Solar Cells on Carrier Recombination in p/i Interface and Bulk Regions", J. M. Pearce, R. J. Koval, A. S. Ferlauto, R. W. Collins, C. R. Wronski, J. Yang, and S. Guha, Applied Physics Letters 77, 3093-3095 (2000).

10. "Recent Advances in Understanding a-Si:H-Based Materials and Performance of Their Solar Cells", C. R. Wronski, L. Jiao, R. J. Koval, and R. W. Collins, Opto-Electronics Review 8, 275-279 (2000).

11. "Ellipsometry in Analysis of Surfaces and Thin Films", R. W. Collins, in: Encyclopedia of Analytical Chemistry, edited by R. A. Myers, (John Wiley & Sons, West Sussex UK, 2000) pp. 9120-9162.

12. "Study of the Amorphous-to-Microcrystalline Transition during Silicon Film Growth at High Rates: Extensions of the Evolutionary Phase Diagram", A. S. Ferlauto, P. I. Rovira, R. J. Koval, C. R. Wronski and R. W. Collins in Amorphous and Heterogeneous Silicon Thin Films - 2000, Materials Research Society Symposium Proceedings, Vol. 609, edited by R. W. Collins, H. M. Branz, S. Guha, H. Okamoto, and M. Stutzmann, (MRS, Pittsburgh, 2000) pp. A2.2.1-6.

13. "Real Time Optics of p-Type Microcrystalline Silicon Deposition on Specular and Textured ZnO-Coated Glass", P. I. Rovira, A. S. Ferlauto, X. Niu, C. R. Wronski, and R. W. Collins, in Amorphous and Heterogeneous Silicon Thin Films - 2000, Materials Research Society Symposium

Proceedings, Vol. 609, edited by R. W. Collins, H. M. Branz, S. Guha, H. Okamoto, and M. Stutzmann, (MRS, Pittsburgh, 2000) pp. A19.6.1-6.

14. "Kinetics of Light-Induced Changes in Protocrystalline Silicon Materials and Devices", R. J. Koval, L. Jiao, X. Niu, Z. Lu, G. Ganguly, J. Yang, S. Guha, R. W. Collins, and C. R. Wronski in Amorphous and Heterogeneous Silicon Thin Films - 2000, Materials Research Society Symposium Proceedings, Vol. 609, edited by R. W. Collins, H. M. Branz, S. Guha, H. Okamoto, and M. Stutzmann, (MRS, Pittsburgh, 2000) pp. A 15.5.1-6.

15. "Exploiting the Thickness-Dependent Amorphous-to-Microcrystalline Phase Transition in the Design of Optimized Amorphous Silicon Solar Cells", R. W. Collins, Joohyun Koh, H. Fujiwara, P. I. Rovira, A. S. Ferlauto, and C. R. Wronski, Technical Digest of the 12th "Sunshine" Workshop on Thin Film Solar Cells, January 2000, Shinjuki, Tokyo, Japan, (MITI-NEDO, Tokyo, 2000), 8 page article.

16. "Alignment and Calibration of the MgF_2 Biplate Compensator for Applications in Rotating-Compensator Multichannel Ellipsometry", Joungchel Lee, P. I. Rovira, Ilsin An, and R. W. Collins, Journal of the Optical Society of America A 18, 1980-1985 (2001).

17. "Dual Rotating-Compensator Multichannel Ellipsometer: Instrument Development for High-Speed Mueller Matrix Spectroscopy of Surfaces and Thin Films", Joungchel Lee, Joohyun Koh, and R. W. Collins, Review of Scientific Instruments 72, 1742-1754 (2001).

18. "Optical Metrology for the Next Generation of a-Si:H-Based Thin Film Photovoltaics", A. S. Ferlauto, G. M. Ferreira, C. Chen, P. I. Rovira, C. R. Wronski, R. W. Collins, X. Deng, and G. Ganguly, in: Photovoltaics for the 21st Century II, edited by R. D. McConnell and V. K. Kapur, (Electrochemical Society, Pennington NJ, 2001), pp. 199 - 228.

19. "Ellipsometry", R. W. Collins in: Encyclopedia of Materials: Science and Technology, (Elsevier Science, Amsterdam, 2001), pp. 2753-2761.

20. "Phase Diagrams for the Optimization of rf Plasma-Enhanced Chemical Vapor Deposition of a-Si:H: Variation in Plasma Power and Substrate Temperature", A. S. Ferlauto, R. J. Koval, C. R. Wronski and R. W. Collins in: Amorphous and Heterogeneous Silicon Thin Films - 2001, Materials Research Society Symposium Proceedings, Vol. 664, edited by M. Stutzmann, J. B. Boyce, J. D. Cohen, R. W. Collins, and J. Hanna, (MRS, Warrendale PA, 2001), pp. A5.4.1-A5.4.6.

21. "Contributions of D^0 and non-D^0 Gap States to the Kinetics of Light-Induced Degradation of Amorphous Silicon under 1 Sun Illumination" J. M. Pearce, X. Niu, R. J. Koval, G. Ganguly, D. E. Carlson, R. W. Collins, and C. R. Wronski, in: Amorphous and Heterogeneous Silicon Thin Films - 2001, Materials Research Society Symposium Proceedings, Vol. 664, edited by M. Stutzmann, J. B. Boyce, J. D. Cohen, R. W. Collins, and J. Hanna, (MRS, Warrendale PA, 2001), pp. A12.3.1-A12.3.6.

22. "Evolution of the Mobility Gap with Thickness in Hydrogen-Diluted Intrinsic Silicon Materials in the Phase Transition Region and its Effect on p-i-n Solar Cell Characteristics", R. J. Koval, J. M. Pearce, A. S. Ferlauto, R. W. Collins, and C. R. Wronski, in: Amorphous and Heterogeneous Silicon Thin Films - 2001, Materials Research Society Symposium Proceedings, Vol. 664, edited by M. Stutzmann, J. B. Boyce, J. D. Cohen, R. W. Collins, and J. Hanna, (MRS, Warrendale PA, 2001), pp. A16.4.1-A16.4.6.

23. "Optical Simulations of the Effect of Transparent Conducting Oxide Interface Layers on Amorphous Silicon Solar Cell Performance", G. M. Ferreira, A. S. Ferlauto, P. I. Rovira, C. Chen, H. V. Nguyen, C. R. Wronski, and R. W. Collins, in: Amorphous and Heterogeneous Silicon Thin

Films - 2001, Materials Research Society Symposium Proceedings, Vol. 664, edited by M. Stutzmann, J. B. Boyce, J. D. Cohen, R. W. Collins, and J. Hanna, (MRS, Warrendale PA, 2001), pp. A24.6.1-A24.6.6.

24. "Insights for Improvement of Silicon-Based Solar Cells from Real Time Optical Studies", R. W. Collins, A. S. Ferlauto, R. J. Koval, J. M. Pearce, P. I. Rovira, and C. R. Wronski, in: Review of Research with Overseas Institutes: Technical Digest, Centennial Memorial Hall, Tokyo Institute of Technology, Tokyo, Japan, (New Energy & Industrial Technology Development Organization, Tokyo, 2001), pp. 1-8.

25. "Evolution of Optoelectronic Properties of Hydrogen Diluted Si:H Materials and their Effect on Solar Cell Characteristics", R. J. Koval, J. M. Pearce, A. S. Ferlauto, J. Koh, R. W. Collins, and C. R. Wronski, in: Review of Research with Overseas Institutes: Technical Digest, Centennial Memorial Hall, Tokyo Institute of Technology, Tokyo, Japan, (New Energy & Industrial Technology Development Organization, Tokyo, 2001), pp. 9-16.

26. "Progress in High Stability Amorphous Silicon Based Solar Cells with Guidance from Real Time Optics", R. W. Collins, A. S. Ferlauto, R. J. Koval, J. M. Pearce, and C. R. Wronski, in: Proceedings of the 2001 National Center for Photovoltaics (NCPV) Program Review Meeting, 14-17 October 2001, Lakewood CO, (NREL Rep. No. EL-520-31065, Golden CO, 2001), pp. 21-22.

27. "Progress in Optical Measurement and Modeling of Multilayer Thin Film Solar Cell Structures", R. W. Collins, G. M. Ferreira, A. S. Ferlauto, C. Chen, C. R. Wronski, X. Deng, and G. Ganguly, in: Proceedings of the 2001 National Center for Photovoltaics (NCPV) Program Review Meeting, 14-17 October 2001, Lakewood CO, (NREL Rep. No. EL-520-31065, Golden CO, 2001), pp. 173-174.

28. "Limitations of Bulk Generation-Recombination on Open Circuit Voltage under 1 Sun Illumination in Amorphous Silicon Solar Cells", J. M. Pearce, R. J. Koval, A. S. Ferlauto, R. W. Collins, and C. R. Wronski, in: Technical Digest of the 12th International Photovoltaic Science and Engineering Conference, (IEEE, New York, 2001), pp. 251-252.

29. "Metastability in Hydrogenated Amorphous Silicon Based Materials and Solar Cells", C. R. Wronski, J. M. Pearce, R. J. Koval, and R. W. Collins, in: Technical Digest of the 12th International Photovoltaic Science and Engineering Conference, (IEEE, New York, 2001), pp. 33-36.

30. "Protocrystalline Phase Transitions in Si:H Materials and their Effect on Solar Cell Characteristics", C. R. Wronski, R. J. Koval, J. M. Pearce, A. S. Ferlauto, J. Koh, and R. W. Collins, in: 11th Workshop on Crystalline Silicon Cell Materials and Processes, (NREL Rep. No. BK-520-30838, Golden CO, 2001), pp. 93-94.

31. "Advances in Plasma-Enhanced Chemical Vapor Deposition of Silicon Films at Low Temperatures", R. W. Collins and A. S. Ferlauto, Current Opinion in Solid State and Material Science 6, 425-437 (2002).

32. "Analytical Model for the Optical Functions of Amorphous Semiconductors from the Near-Infrared to Ultraviolet: Applications in Thin Film Photovoltaics", A. S. Ferlauto, G. M. Ferreira, J. M. Pearce, C. R. Wronski, R. W. Collins, Xunming Deng, and Gautam Ganguly, Journal of Applied Physics 92, 2424-2436 (2002).

33. "Maximization of the Open Circuit Voltage for Hydrogenated Amorphous Silicon n-i-p Solar Cells by Incorporation of Protocrystalline p-Layers", R. J. Koval, C. Chen, G. M. Ferreira, A. S. Ferlauto, J. M. Pearce, P. I. Rovira, C. R. Wronski, and R. W. Collins, Applied Physics Letters 81, 1258-1260 (2002).

34. "Phase Diagrams for Si:H Film Growth by Plasma-Enhanced Chemical Vapor Deposition", A. S. Ferlauto, R. J. Koval, C. R. Wronski, and R. W. Collins, Journal of Non-Crystalline Solids 299, 68-73 (2002).

35. "Mobility Gap Profiles in Si:H Intrinsic Layers Prepared by H_2-Dilution of SiH_4: Effects on the Performance of p-i-n Solar Cells", R. J. Koval, A. S. Ferlauto, J. M. Pearce, C. R. Wronski, and R. W. Collins, Journal of Non-Crystalline Solids 299, 1136-1141 (2002).

36. "Extended Phase Diagrams for Guiding Plasma-Enhanced Chemical Vapor Deposition of Silicon Thin Films for Photovoltaic Applications", A. S. Ferlauto, R. J. Koval, C. R. Wronski, and R. W. Collins, Applied Physics Letters 80, 2666-2668 (2002).

37. "Thickness Evolution of the Microstructural and Optical Properties of Si:H Films in the Amorphous-to-Microcrystalline Phase Transition Region", A. S. Ferlauto, G. M. Ferreira, R. J. Koval, J. M. Pearce, C. R. Wronski, R. W. Collins, M. M. Al-Jassim, and K. M. Jones, Conference Record of the 29th Photovoltaic Specialists Conference, May 2002, New Orleans, LA (IEEE, New York, 2002, in press).

38. "Correlation of Light-Induced Changes in a-Si:H Films with Characteristics of Corresponding Solar Cells", J. M. Pearce, R. J. Koval, R.W. Collins, C. R. Wronski, M. M. Al-Jassim, and K. M. Jones, Conference Record of the 29th Photovoltaic Specialists Conference, May 2002, New Orleans, LA (IEEE, New York, 2002, in press).

39. "Microstructurally Engineered p-Layers for Obtaining High Open-Circuit Voltages in a-Si:H n-i-p Solar Cells", R. J. Koval, J. M. Pearce, Chi Chen, G. M. Ferreira, A. S. Ferlauto, R. W. Collins, and C. R. Wronski, Conference Record of the 29th Photovoltaic Specialists Conference, May 2002, New Orleans, LA (IEEE, New York, 2002, in press).

40. "Protocrystalline Si:H p-Type Layers for Maximization of the Open Circuit Voltage in a-Si:H n-i-p Solar Cells", R. J. Koval, Chi Chen, G. M. Ferreira, A. S. Ferlauto, J. M. Pearce, P. I. Rovira, C. R. Wronski, and R. W. Collins, Materials Research Society Symposium Proceedings, (MRS, Warrendale PA, 2002, in press).

41. "Light Induced Defect Creation Kinetics in Thin Film Protocrystalline Silicon Materials and Their Solar Cells", C. R. Wronski, R. W. Collins, J. M. Pearce, R. J. Koval, X. Niu, A. S. Ferlauto and J. Koh, Materials Research Society Symposium Proceedings, (MRS, Warrendale PA, 2002, in press).

42. "Evolution of Crystallinity in Mixed-Phase (a+□c)-Si:H as Determined by Real Time Spectroscopic Ellipsometry", A. S. Ferlauto, G. M. Ferreira, R. J. Koval, J. M. Pearce, C. R. Wronski, and R. W. Collins, Materials Research Society Symposium Proceedings, (MRS, Warrendale, 2003, submitted).

43. "Optical Functions of Transparent Conductors and their Impact on Collection in Amorphous Silicon Solar Cells", G. M. Ferreira, Chi Chen, Ilsin An, C. R. Wronski, R. W. Collins, G. Ganguly, Joong Hwan Kwak, and Keong Su Lim, Materials Research Society Symposium Proceedings, (MRS, Warrendale, 2003, submitted).

44. "Application of Deposition Phase Diagrams for the Optimization of a-Si:H-Based Materials and Solar Cells", R. W. Collins, A. S. Ferlauto, G. M. Ferreira, Chi Chen, R. J. Koval, J. M. Pearce, and C. R. Wronski, Materials Research Society Symposium Proceedings, (MRS, Warrendale, 2003, submitted).

45. "Optical Physics of Materials", R. W. Collins and A. S. Ferlauto, in Handbook of Ellipsometry, edited by H. G. Tompkins and E. A. Irene (Noyes, Boston, 2003, in press).

46. "Multichannel Ellipsometry", R. W. Collins, Ilsin An, Joungchel Lee, and J. A. Zapien, in Handbook of Ellipsometry, edited by H. G. Tompkins and E. A. Irene (Noyes, Boston, 2003, in press).

47. "Analysis of Optical Anisotropy in Reflecting Surfaces by Multichannel Mueller Matrix Ellipsometry", Chi Chen, Ilsin An, J. A. Zapien, and R. W. Collins, Review of Scientific Instruments (submitted, 2003).

48. "Multichannel Mueller Matrix Ellipsometry for Simultaneous Real Time Measurement of Bulk Isotropic and Surface Anisotropic Complex Dielectric Functions of Semiconductors", Chi Chen, Ilsin An, and R. W. Collins, Physical Review Letters **90**, 217402 (2003).

49. "Ellipsometry", R. W. Collins, Optics Encyclopedia (VCH, New York, submitted, 2003).

50. "Uniform Distribution of Defects in Intrinsic Layers of a-Si:H Solar Cells: Evidence from Forward Bias Current-Voltage Characteristics", J. Deng, J. M. Pearce, R. J. Koval, V. Vlahos, R. W. Collins and C. R. Wronski, Applied Physics Letters (submitted, 2003).

51. "Evolution of Microstructure and Phase in Amorphous, Protocrystalline, and Microcrystalline Silicon Studied by Real Time Spectroscopic Ellipsometry, R. W. Collins, A. S. Ferlauto, G. M. Ferreira, C. Chen, J. Koh, R. J. Koval, Y. Lee, J. M. Pearce, and C. R. Wronski, Solar Energy Materials and Solar Cells (in press, 2003).

Edited Books

"Amorphous and Heterogeneous Silicon Thin Films - 2000", Materials Research Society Symposium Proceedings, Vol. 609, edited by R. W. Collins, H. M. Branz, S. Guha, H. Okamoto, and M. Stutzmann, (Materials Research Society, Pittsburgh, 2000) pp. 1-1075.

"Amorphous and Heterogeneous Silicon Thin Films - 2001", Materials Research Society Symposium Proceedings, Vol. 664, edited by M. Stutzmann, J. B. Boyce, J. D. Cohen, R. W. Collins, and J. Hanna, (Materials Research Society, Pittsburgh, 2001).

REPORT DOCUMENTATION PAGE

Form Approved
OMB NO. 0704-0188

Public reporting burden for this collection of information is estimated to average 1 hour per response, including the time for reviewing instructions, searching existing data sources, gathering and maintaining the data needed, and completing and reviewing the collection of information. Send comments regarding this burden estimate or any other aspect of this collection of information, including suggestions for reducing this burden, to Washington Headquarters Services, Directorate for Information Operations and Reports, 1215 Jefferson Davis Highway, Suite 1204, Arlington, VA 22202-4302, and to the Office of Management and Budget, Paperwork Reduction Project (0704-0188), Washington, DC 20503.

1. AGENCY USE ONLY (Leave blank)	2. REPORT DATE October 2003	3. REPORT TYPE AND DATES COVERED Subcontract Report 1 August 1999–12 August 2002

4. TITLE AND SUBTITLE
Real Time Optics of the Growth of Textured Silicon Films in Photovoltaics: Final Technical Report, 1 August 1999–12 August 2002

5. FUNDING NUMBERS
PVP32601
AAD-9-18668-09

6. AUTHOR(S)
R.W. Collins and C.R. Wronski

7. PERFORMING ORGANIZATION NAME(S) AND ADDRESS(ES)
Materials Research Institute
The Pennsylvania State University
University Park, Pennsylvania 16802

8. PERFORMING ORGANIZATION REPORT NUMBER

9. SPONSORING/MONITORING AGENCY NAME(S) AND ADDRESS(ES)
National Renewable Energy Laboratory
1617 Cole Blvd.
Golden, CO 80401-3393

10. SPONSORING/MONITORING AGENCY REPORT NUMBER
NREL/SR-520-34823

11. SUPPLEMENTARY NOTES
NREL Technical Monitor: Richard Matson

12a. DISTRIBUTION/AVAILABILITY STATEMENT
National Technical Information Service
U.S. Department of Commerce
5285 Port Royal Road
Springfield, VA 22161

12b. DISTRIBUTION CODE

13. ABSTRACT *(Maximum 200 words):* Novel optical instruments, including single and dual rotating-compensator multichannel ellipsometers, have been designed and developed to probe the evolution of the microstructure, spectroscopic optical properties, and other materials characteristics during the fabrication and processing of individual thin films and thin-film structures used in photovoltaic devices. These instruments provide a foundation for next-generation process design/control and metrology in existing and future photovoltaics technologies. In this project, the materials system studied in the greatest detail was thin-film silicon, fabricated at low temperatures by plasma-enhanced chemical vapor deposition. Real-time measurements of such thin films by multichannel ellipsometry have established deposition phase diagrams that provide guiding principles for multistep fabrication of high-performance amorphous (a-Si:H) and microcrystalline (μc-Si:H) solar cells. Such phase diagrams have also served to disprove conventional wisdom in the fabrication of thin-film solar cell structures, thus avoiding future unproductive research efforts.

In addition, a combination of the novel real-time and ex-situ optical measurements have provided databases of analytical formulas for the spectroscopic optical properties of thin film and bulk materials used in amorphous and microcrystalline silicon thin-film photovoltaics technologies. Such databases include, for example, amorphous silicon-based alloys of any pre-specified optical bandgap, the transparent conducting oxide (TCO) films and superstrate glasses used by industry, and the metallic retro-reflecting materials. This database can be applied in optical modeling of the device structures used in these technologies, and in next-generation optical engineering for maximum collection of incident solar irradiance. As examples of the approach, we have highlighted how microscopic roughness at the TCO/p-layer interface acts as an antireflecting layer for enhanced collection in p-i-n structures and how intermixing at the ZnO/Ag interface in retro-reflectors act as a parasitic absorber for reduced collection.

14. SUBJECT TERMS: PV; rotating-compensator multichannel ellipsometers; microstructure; spectroscopic optical properties; thin film; plasma-enhanced chemical vapor deposition; solar cells; amorphous silicon; microcrystalline silicon; transparent conducting oxide (TCO); metallic retro-reflecting; parasitic absorber

15. NUMBER OF PAGES

16. PRICE CODE

17. SECURITY CLASSIFICATION OF REPORT	18. SECURITY CLASSIFICATION OF THIS PAGE	19. SECURITY CLASSIFICATION OF ABSTRACT	20. LIMITATION OF ABSTRACT
Unclassified	Unclassified	Unclassified	UL